

CROSS CORRELATIONS OF THE COSMIC INFRARED BACKGROUND

PENGJIE ZHANG
zhangpj@fnal.gov

NASA/Fermilab Astrophysics Group, Fermi National Accelerator Laboratory, Box 500, Batavia, IL 60510

Draft version November 5, 2018

ABSTRACT

The cosmic infrared background (CIB) is a sensitive measure of the star formation history. But this background is overwhelmed by foregrounds, which bias the CIB mean flux and auto correlation measurement severely. Since dominant foregrounds do not correlate with the large scale structure, the cross correlation of CIB with galaxies is free of such foregrounds and presents as an unbiased measure of the star formation history. In such cross correlation measurement, one can utilize all frequency information, instead of being limited to several narrow frequency windows. This allows the measurement of CIB based on integrated intensity, whose theoretical prediction is based on energy conservation, thus is fairly model independent and robust. The redshift information of CIB sources can be directly recovered with the aid of galaxy photometric redshifts. In the far IR region, correlation signal is around 10% at degree scale. Combining FIRAS and SDSS, the cross correlation can be measured with 20% accuracy (statistical and systematics errors) at $l \sim 40$. Such measurement would allow the measurement of star formation rate with comparable accuracies to $z \sim 1$. Future CIB experiments with 1° resolution are able to measure the star formation rate with 10% accuracy to $z \sim 1.5$. Secondary CMB anisotropies arising from the large scale structure correlate with CIB. The correlation strength is about $0.5\mu\text{K}$ at $\sim 10^\circ$ (the integrated Sachs-Wolfe effect) and $\sim -0.3\mu\text{K}$ at $\sim 1^\circ$ (the Sunyaev Zeldovich effect, Rayleigh-Jeans regime). FIRAS+WMAP would allow the measurement of the ISW effect with $\gtrsim 5\sigma$ confidence. Its detection helps to constrain the amount of dark energy and far IR emissivity bias. A future CIB experiment with better angular resolution would allow the measurement of CIB-SZ cross correlation and help to understand the effect of SN feedback on the SZ effect.

Subject headings: cosmology: large scale structure; infrared: theory–diffuse background; star: formation

1. INTRODUCTION

Detections of the cosmic infrared background (CIB) (refer to Hauser & Dwek (2001) for a recent review) open a new window for the study of star formation history. The main CIB component associates with star formation. Dust in extragalactic galaxies absorbs UV photons and reemits in far infrared region. Cosmic expansion shifts light emitted by low mass population I/II stars or massive population III stars into near infrared region. We denote this CIB originated from star formation as SCIB, which provides a fairly unbiased and statistically robust measure of the star formation history (SFH). But the precision CIB measurement is challenged by overwhelming foregrounds. Interplanetary dust emission dominates over the CIB by an order of magnitude at $\lambda \lesssim 100\mu\text{m}$. Galactic interstellar dust emission peaks at $\lambda \sim 100\mu\text{m}$ with an intensity at least comparable to the CIB. Bright galactic sources such as stars and faint galactic sources have intensities at least several times larger than the CIB in near IR region. The CMB dominates over the $\lambda \gtrsim 400\mu\text{m}$ far IR region.

To reliably separate the CIB and these dominant foregrounds, robust understanding of foreground spacial and spectral distribution is required. The removal of these foregrounds has enabled successful CIB detections. But the residual foregrounds still cause large dispersions in the current CIB intensity measurements (see table 1 of Hauser & Dwek (2001) for a review up to 2001 and Wright (2003) and reference therein for a recent compilation of COBE data).

One way to bypass foregrounds is to investigate the

CIB fluctuations, as proposed by Bond, Carr, & Hogan (1986); Haiman & Knox (2000); Knox, Cooray, Eisenstein, & Haiman (2001). This fluctuation approach has several advantages. (1) The CIB roughly follows star forming galaxy (SFG) distribution, so one expects $\sim 10\%$ fluctuations at degree scale, which are about 4 orders of magnitude larger than the CMB fluctuations. (2) Fluctuations of galactic foregrounds concentrate on large angular scales, for example, the power spectrum of the galactic interstellar medium emission scales as $C_l \propto l^{-3}$ (Wright 1998). Thus at sufficiently small angular scales, The CIB fluctuations exceed these foreground fluctuations.

But correlations of CIB foregrounds bias this approach. Fluctuations of Galactic interstellar dust emission dominate over the CIB intrinsic fluctuations in a large sky fraction and large frequency and angular ranges (Knox, Cooray, Eisenstein, & Haiman 2001). The CIB auto correlation measurement in such regions requires an accurate removal of these foreground correlations. The residual foreground correlations bias the intrinsic CIB auto correlation measurement and the following extraction of SFH. This problem is most severe at large angular scale ($l \lesssim 200$) or short wavelength ($\lambda \lesssim 300\mu\text{m}$) and may affect the estimation of Knox, Cooray, Eisenstein, & Haiman (2001) significantly. To minimize such bias, the auto correlation measurement has to be limited to finite sky regions, frequency bands and angular scales. These limitations increase the sample variance.

For the purpose of extracting star formation rate (SFR),

various non-stellar CIB, such as AGN CIB¹, introduce extra systematic errors. AGNs have similar clustering property as galaxies and similar thermal emission features as extragalactic dust, so it is hard to separate AGN CIB and SCIB by the mean flux and auto correlation measurements, even utilizing multi-frequency information. Since AGN may contribute $\sim 10\%$ to the CIB intensities (Hauser & Dwek (2001) and reference therein), it may introduce $\sim 10\%$ systematic error to the SFR measurement.

The ultimate challenge of the auto correlation approach is to recover the redshift information of CIB sources. This can be done by multi-band CIB correlations (Knox, Cooray, Eisenstein, & Haiman 2001). But such approach requires detailed understanding of dust composition and size distribution and UV sources distribution, such modeling is difficult and uncertainty it introduces is hard to quantify.

With all these concerns, new CIB analysis method is demanded. Dominant CIB foregrounds such as galactic foregrounds and primary CMB do not correlate with extragalactic galaxies. This suggests that crossing correlating the CIB with galaxies may alleviate foreground contaminations. Residual correlations originated from other CIB and extragalactic contaminations are negligible comparing to the SCIB-galaxy correlation. Though AGN CIB-galaxy cross correlation still exists in such approach and could bias the result, its effect is at most $\sim 10\%$. Furthermore, one can utilize the difference of AGN redshift distribution versus that of SFGs to at least partially separate the AGN contribution. Thus, the cross correlation measurement of the CIB and galaxies is fairly unbiased. With the aid of galaxy photometric redshift information, one does not need to rely on frequency information to recover redshift information of CIB sources. We only need to model the integrated CIB intensity, whose prediction is directly based on energy conservation and thus fairly robust. So the cross correlation of CIB with galaxies would avoid most problems in the mean flux and auto correlation approaches.

Since dust emission in far IR region is directly related to SFR, throughout this paper, we focus on the far IR region. Similar method can be applied to near IR region, which will constrain SFR at low mass end. In §2, we estimate the auto and cross correlation power spectra of SCIB based on the integrated CIB intensity. Our model can be applied to CIB-lensing cross correlation, as Song, Cooray, Knox, & Zaldarriaga (2003) did. But weak lensing surveys are limited by finite sky coverage while redshift information of lenses is entangled, so we postpone such calculation. We investigate the observational feasibility of such cross correlation by estimating the systematic errors (§3.1) and the statistical errors (§3.2). Since the SCIB traces the large scale structure, it correlates with secondary CMB anisotropies such as the integrated Sachs-Wolfe (ISW) effect and the thermal Sunyaev-Zeldovich (SZ) effect. The cross correlation of the CIB and the CMB provides another way to constrain dark energy and the large scale structure. We predict the strength of such correlation in §4. Our predictions are based on the WMAP-alone cosmology with $\Omega_m = 0.268$, $\Omega_\Lambda = 1 - \Omega_m$, $\Omega_b = 0.044$,

$\sigma_8 = 0.84$ and $h = 0.71$ (Spergel et al. 2003)².

2. INTRINSIC COSMIC INFRARED BACKGROUND FLUCTUATIONS

We model the SCIB based on energy conservation. Observations suggest that $f_{\text{absorption}} \sim 90\%$ UV light is absorbed by dust (Massarotti, Iovino, & Buzzoni (2001) and reference therein) and reemitted in far IR. Since UV emission is dominated by short-life O/B stars, UV emissivity ρ_{UV} is directly related to SFR by

$$\rho_{UV}(\nu) = \alpha_\nu \frac{\text{SFR}}{M_\odot \text{yr}^{-1}}. \quad (1)$$

Coefficient α_ν is determined by the initial mass function (IMF). It strongly depends on the shape of IMF at high mass end. At 1500 \AA , for the Salpeter IMF, $\alpha_\nu \simeq 8.0 \times 10^{-25} \text{ nW Hz}^{-1}$ (Madau, Pozzetti, & Dickinson 1998). For the Scalo IMF which has much less massive stars, α_ν is about twice smaller. Since the Scalo IMF produces too red integrated galaxy spectra (Lilly, Le Fevre, Hammer, & Crampton 1996) and too low CIB intensity, we consider only the Salpeter IMF in this paper. For the Salpeter IMF, α_ν has only a weak dependence on ν . For example, at 2800 \AA , $\alpha_\nu \simeq 7.9 \times 10^{-25} \text{ nW Hz}^{-1}$. Then the integrated dust FIR emissivity is given by

$$\bar{j}_d = \alpha f_{\text{absorption}} \frac{\text{SFR}}{M_\odot \text{yr}^{-1}}. \quad (2)$$

Here, $\alpha = \int_{UV} \alpha_\nu d\nu \simeq 1.6 \times 10^{-9} \text{ nW}$. The integrated SCIB intensity at direction \hat{n} is

$$I(\hat{n}) = \int \frac{\bar{j}_d(1 + \delta_j(\chi, \hat{n}))}{4\pi(1+z)^2} d\chi. \quad (3)$$

Here, δ_j is the fractional fluctuation of the integrated IR emissivity. χ is the comoving distance. SFR at $z \lesssim 1.2$ is relatively robustly measured and we adopt it as $\text{SFR}(z) = 10^{-2.1} \exp(t/2.6 \text{ Gyr}) M_\odot \text{yr}^{-1} \text{ Mpc}^{-3}$ (Hippelein et al. 2003). Here, t is the look-back time. For $z > 1.2$, we consider three SFR:

$$\begin{aligned} \text{SFR}(z = 1.2) \exp\left(-\frac{t - t(z = 1.2)}{2.5 \text{ Gyr}}\right) &: \text{SFR1} \\ \text{SFR}(z = 1.2) &: \text{SFR2} \end{aligned} \quad (4)$$

$$10^{-2.1} \exp\left(\frac{t}{2.6 \text{ Gyr}}\right) M_\odot \text{yr}^{-1} \text{ Mpc}^{-3} : \text{SFR3} .$$

For the Salpeter IMF, we obtain $\bar{I} \simeq 16, 20, 30 \text{ nW m}^{-2} \text{ sr}^{-1}$, respectively. These results are consistent with observations, but due to the large dispersion in the observational results (see Hauser & Dwek (2001); Wright (2003) for reviews), no specific conclusion can be drawn.

We calculate the CIB fluctuations by the Limber's equation:

$$\frac{l^2}{2\pi} C_{\text{IR}} \bar{I}^2 = \pi \int \left(\frac{\bar{j}_d}{4\pi(1+z)^2} \right)^2 \frac{\chi}{l} \Delta_j^2 \left(\frac{l}{\chi}, z \right) d\chi, \quad (5)$$

$$\frac{l^2}{2\pi} C_{\text{IR,G}} \bar{I} \bar{\Sigma}_G = \int_{z_1}^{z_2} \frac{\bar{j}_d}{4(1+z)^2} \frac{\chi}{l} \Delta_{jG}^2 \left(\frac{l}{\chi}, z \right) \frac{dn}{dz} dz. \quad (6)$$

Here, Δ_j^2 and Δ_{jG}^2 are the variances (power spectra) of δ_j and its cross correlation with galaxy number overdensity δ_G , respectively. $dn/dz(z)$ is the

¹ We always refer AGN CIB as the CIB contributed by AGN accretion.

² For simplicity, we adopt a slightly different Ω_Λ from the best fit value $1.02 - \Omega_m$. This change has negligible effect on our results.

galaxy number distribution function in a given galaxy survey. The galaxy surface density is defined as $\Sigma_G = \int dn/dz(1 + \delta_G)dz$. We adopt the parametric form $dn/dz = 3z^2/2/(z_m/1.412)^3 \exp(-(1.412z/z_m)^{1.5})$ (Baugh & Efstathiou 1993). z_m is the median redshift of the galaxy distribution. For SDSS, We $z_m \sim 0.5$ (Dodelson et al. 2002). The above equations hold at angular scales $\lesssim 30^\circ$ or $l \gtrsim 10$. For smaller l , one has to calculate the spherical Bessel integral. Since the small l modes are dominated by cosmic variance and/or foregrounds, whose power concentrates on large angular scales, we neglect the calculation for such small l .

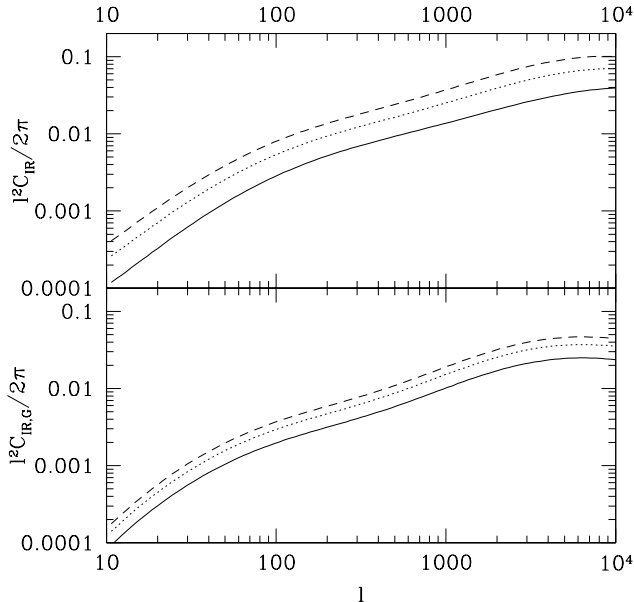


FIG. 1.— The CIB power spectra. The top panel plots the CIB auto correlation power spectra while the bottom panel plots the cross correlation power spectra with SDSS galaxies. We assume three SFR: SFR1 (dash lines), SFR2 (dot lines) and SFR3 (solid lines). The change of amplitude reflects the change of redshift where the dominant correlation signal comes from.

Δ_j^2 and Δ_{jG}^2 are generally unknown. Since dust associates with SFGs, averaging over many galaxies, j_d should trace SFG distribution, which in turn traces dark matter distribution. A 10^2 sky area contains more than 100 SFGs, so one expects that the constant bias assumption $\delta_j = b_j \delta_{DM}$ applies at $\gtrsim 3'$ scale. In principle, b_j is an observable and can be inferred from the combined CIB mean flux and correlation measurements (§3.2) or from the CIB-ISW cross correlation measurement (§4). For simplicity, we assume $b_j = b_{SFG} = 3$ (Haiman & Knox 2000). This SFG bias is inferred from Lyman break galaxies (Giavalisco et al. 1998). The dark matter power spectrum is calculated by the code of Smith et al. (2003).

The fractional fluctuations at degree scales are about 10% at degree scale, which translate to intensity fluctuations $\sim 2 \text{ nW m}^{-2} \text{ sr}^{-1}$. These fluctuations are consistent with both theoretical predictions (Haiman & Knox 2000; Knox, Cooray, Eisenstein, & Haiman 2001) and observations (Hauser & Dwek 2001; Miville-Deschênes, Lagache, & Puget 2002).

3. ERROR ESTIMATION

The above prediction assumes that the observational wavelength band contains all extragalactic dust emission. The requirement on the wavelength band can be estimated as follows. Extragalactic dust emission can be described by a gray-body spectrum $I_\nu \propto \nu^\beta B_\nu(T)$ with typical $T \sim 20 \text{ K}$ (see, e.g., Haiman & Knox (2000)) and $\beta = 2$ (Draine & Lee 1984). Here, $B_\nu(T)$ is the Planck function. νI_ν peaks at $\simeq 2.5T/20\text{K}$ THz (or, equivalently, $20\text{K}/T120\mu\text{m}$). More than 96% emission comes from the range $[0.8, 5]T/20\text{K}$ ($[60, 375]20\text{K}/T\mu\text{m}$). Since star formation rate was more than an order of magnitude higher at $z \sim 1$ than at present, considering the redshift effect, an integral range $[0.3, 3]$ THz ($[100, 1000]\mu\text{m}$) should contain almost all contribution from extragalactic dust emission. Indeed, from the fitted FIRAS far infrared background (FIRB) spectrum (Fixsen et al. 1998)

$$I_\nu = 1.3 \pm 0.4 \times 10^{-5} \left(\frac{\nu}{3\text{THz}} \right)^{0.64 \pm 0.12} B_\nu(18.5 \pm 1.2\text{K}), \quad (7)$$

this fraction is $\gtrsim 92\%$. This frequency range may underestimate low redshift contribution by 10%, but it contains $\gtrsim 95\%$ extragalactic dust emission from $z \gtrsim 0.6$ and is sufficient for our extraction of SFR at $z \sim 1$.

FIRAS satisfies this wavelength band requirement, so we take it as our target to estimate both the statistical and systematic errors of the cross correlation measurement. The assumption that $[0.3, 3]$ THz contains all dust emission would introduce several percent errors at low redshift, which are minor comparing to other systematic errors (§3.1).

3.1. Systematics errors

Non-stellar CIB sources, if correlate with large scale structure, bias SFR measured from the CIB-galaxy cross correlation. In this section, we estimate the systematic errors caused by such sources. We find that the dominant systematic error comes from AGN CIB, which may contribute 10% to the cross correlation. We show that AGN CIB can be at least partially subtracted. In the worst case that these sources are not subtractive, they can introduce at most 10% systematic error to the measured j_d , which is still quite accurate comparing to current SFR measurement (see, e.g. Hippelein et al. (2003) for recent data compilation).

3.1.1. AGN

AGN may contribute $\sim 10\%$ to the CIB flux through the thermal emission of dust heated by the central black hole (Hauser & Dwek (2001) and reference therein). This non-stellar AGN contribution would affect the determination of SFR by a comparable fraction. AGNs have similar clustering property as galaxies and similar thermal emission feature as extragalactic dust, so it is hard to separate AGN CIB and SCIB by the mean flux and auto correlation measurements, even with the aid of multi-frequency information. Many high redshift AGNs present as luminous infrared galaxies and dominate $L_{IR} > 10^{11} L_\odot$ object catalog (Sanders & Mirabel 1996). So point source identification, at least at high luminosity end, may be feasible and help to understand the contribution of AGNs. But the

distinguishing of energy sources of such IR emission, gravitational potential energy or nuclear energy, is not very clear ((Hauser & Dwek 2001) and reference therein).

AGN contamination can be partially cleaned by cross correlation with galaxies.

- Dust heated by starbursts has temperature $T \sim 20\text{K}$ while dust associated with AGN IR emission has temperature $T \sim 60\text{-}100\text{K}$ (Haas et al. 1998). Since the observed Far IR CIB corresponds to gray-body radiation with $T \sim 18\text{K}$, the AGN CIB mainly comes from high redshifts. Utilizing the redshift information obtained from the cross correlation with galaxies, AGN contamination could be localized to high z .
- AGN-late type galaxy cross correlation is much weaker than AGN-early type galaxy cross correlation at arc minute scale (Brown, Boyle, & Webster 2001) while SFGs strongly correlate with late type galaxies. For future CIB survey which can resolve this scale, one can distinguish the contribution of AGN by cross correlating CIB with early and later type galaxies separately.

3.1.2. The integrated Sachs-Wolfe effect

The time variation of gravitational potential field introduces secondary CMB temperature fluctuations (Sachs & Wolfe 1967):

$$\Theta_{\text{ISW}} \equiv \frac{\delta T}{T_{\text{CMB}}} = 2 \int \frac{\dot{\phi}}{c^2} a \frac{d\chi}{c}. \quad (8)$$

If the variation of gravitational potential ϕ is caused by the deviation from a $\Omega_m = 1$ universe, this effect is called the integrated Sachs-Wolfe (ISW) effect. The contribution of the ISW effect to CIB intensity is

$$I_{\text{ISW}} = \Theta_{\text{ISW}} \int_{\text{FIR}} \frac{\partial I_\nu}{\partial \nu} d\nu \simeq \Theta_{\text{ISW}} 0.2 \text{ nW m}^{-2} \text{ sr}^{-1}. \quad (9)$$

The temperature fluctuation caused by ISW $\delta\Theta_{\text{ISW}}$ is $\lesssim 10^{-5}$, so fluctuations of the CIB caused by ISW are $\sim 10^{-6} \text{ nW m}^{-2} \text{ sr}^{-1}$. We then can safely neglect this effect.

3.1.3. The thermal Sunyaev-Zeldovich effect

Free electrons scatter off CMB photons by their thermal motions and introduce secondary CMB temperature fluctuations, namely, the thermal Sunyaev-Zeldovich (SZ) effect. It contributes an intensity I_{SZ} to the CIB (Zeldovich & Sunyaev 1969)

$$I_{\text{SZ}} = -2y \int_{\text{FIR}} \frac{x \exp(x)}{\exp(x) - 1} \left(2 - \frac{x/2}{\tanh(x/2)} \right) d\nu \quad (10)$$

$$\sim y 10^3 \text{ nW m}^{-2} \text{ sr}^{-1}.$$

Here $x \equiv h\nu/k_B T_{\text{CMB}}$. Since electron thermal energy is much higher than CMB photon energy, photons gain energy and shift toward infrared frequency after scattering. So the SZ contribution to the CIB is much larger than that of the ISW effect.

The y parameter is given by the integral of electron thermal pressure p_e along the line of sight

$$y = \int \frac{n_e k_B T_e}{m_e c^2} \sigma_T a d\chi \equiv \int \frac{p_e}{m_e c^2} \sigma_T a d\chi. \quad (11)$$

The fluctuation of y is $\sim 10^{-6}$ at degree scale (see, e.g., Zhang & Pen (2001); Zhang, Pen, & Wang (2002)). Then fluctuations it introduces to the CIB are $\sim 10^{-3} \text{ nW m}^{-2} \text{ sr}^{-1}$, which are still ~ 1000 times smaller than SCIB fluctuations and can be neglected.

3.1.4. Brown dwarfs

Brown dwarfs associate with galaxies, so the CIB caused by brown dwarfs has fractional fluctuations of the same order as the SCIB. Since the total mass of brown dwarfs accounts for $\ll 1\%$ of the total energy in the universe, its contribution to CIB intensity is $\ll 0.01 \text{ nW m}^{-2} \text{ sr}^{-1}$ (Karimabadi & Blitz 1984). So its contribution to CIB fluctuations is at most $\sim 0.1\%$ of SCIB fluctuations and can be neglected.

3.1.5. Intergalactic dust

Intergalactic dust correlates with galaxies. The CIB contributed by intergalactic dust should have similar fractional fluctuation as the SCIB. But the contribution of intergalactic dust to the CIB flux seems to be negligible based on SCUBA measurement (see Hauser & Dwek (2001) and reference therein for detailed discussion). The existence of abundant intergalactic dust would dim far-away SNIas and alter the conclusion of accelerating expansion of the universe based on SNIa Hubble diagram. Since WMAP has independently confirmed the acceleration of the expansion of the universe without SNIa prior (Spergel et al. 2003), there is little room left for intergalactic dust. So we will neglect this possible source.

3.1.6. Other cosmic sources

Bond, Carr, & Hogan (1986) discussed several other possible CIB sources. Primeval galaxies, first stars and decaying particles all reside at very high redshifts. Gravitational lensing caused by low z dark matter (shallower than the corresponding galaxy survey) correlate the high z emission with low z galaxies. But such correlation is negligible due to two reasons. Firstly, the correlation is caused by low z dark matter lensing. For example, the cross correlation with SDSS would be mainly caused by dark matter at $z \sim z_m/2 = 0.2$. So the lensing effect is small. Secondly, these high z CIB sources only contribute a small fraction, if not negligible, to the total CIB intensity.

3.1.7. Contaminations of galaxy surveys

Galactic dust causes extinction, which biases the observed galaxy distributions. This effect may correlate the galactic dust foregrounds of CIB with extragalactic galaxies. But since at least the first order effect of extinction is included in the observed galaxy number distribution dn/dz , one expects the residual correlation caused by dust extinction to be negligible. Stellar contamination in galaxy surveys also correlate CIB foregrounds with galaxy distribution. But such contamination is at 1% level (e.g. SDSS, Sheldon et al. (2003)) and is thus negligible, too.

3.2. Statistical errors

The statistical errors of $C_{\text{IR,G}}$ measurement are

$$\frac{\Delta(C\bar{I}\bar{\Sigma}_G)}{C\bar{I}\bar{\Sigma}_G} = \sqrt{\frac{1 + (C_{\text{IR}} + C_{\text{dust}} + \frac{C_{\text{short}}}{W_l^2})(C_G + \frac{C_{N,G}}{W_l^2})C_{\text{IR,G}}^{-2}}{(2l+1)\Delta l f_{\text{sky}}}} \quad (12)$$

In this expression, we have assumed Gaussian fluctuations in the CIB, which should at least hold at degree or larger scales. In the [0.3, 3] THz frequency range, the integrated CMB intensity fluctuation is negligible. We consider two dominant noise sources: interplanetary and galactic dust, and short noise of the signal. We adopt $C_{\text{dust}} = (10 \text{ nWm}^{-2}\text{sr}^{-1})^2 l^{-3}$. The l dependence is adopted from Wright (1998) and the amplitude roughly corresponds to the case avoid of the galactic plane (Wright 1998). The short noise power spectrum is estimated by $C_{\text{short}} = 4\pi/N_{\text{SFG}}$. In this expression, we have omitted the flux variation of individual SFG. We further assume the total number of SFG to be $N_{\text{SFG}} = 2 \times 10^9$. The window function W_l reflects the angular resolution of the CIB survey. We approximate it as a Gaussian function $W_l = \exp(-l^2\theta_0^2/2)$ with $\theta_0 = \text{FWHM}/(2\sqrt{2\ln 2})$. While the FIRAS beam FWHM is nominally 7° across it has sharper edges than a Gaussian beam so for many applications it is better approximated by a Gaussian beam with 5° FWHM³. $C_{N,G} = 4\pi f_{\text{sky}}/N_G$ is the Poisson noise of a galaxy survey. We adopt the expected number of SDSS galaxies as $N_G = 5 \times 10^7$ and choose $f_{\text{sky}} = 1/4$. The bin size Δl is chosen to be $\Delta l = 0.5l$.

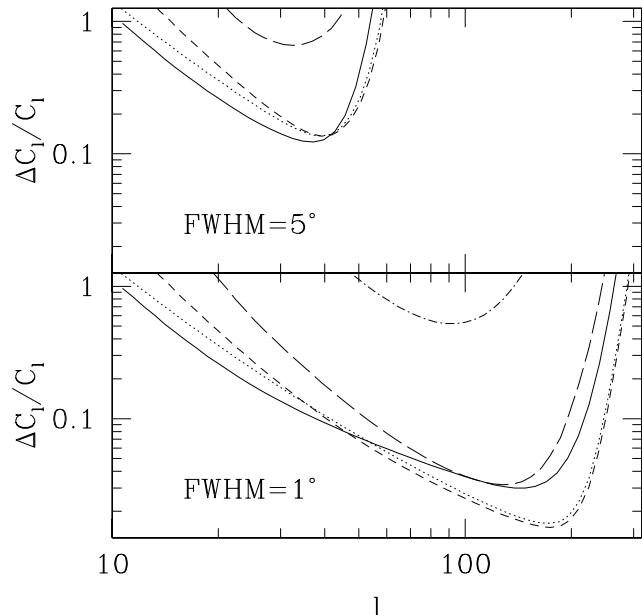


FIG. 2.— The statistical errors in the CIB-galaxy correlation measurement. The redshift bins adopted are: $[0, \infty]$ (solid line), $[0.0, 0.2]$ (dot line), $[0.4, 0.6]$ (short dash line), $[1.0, 1.2]$ (long dash line) and $[1.6, 1.8]$ (dot-dash line). The top panel corresponds to FIRAS+SDSS and the bottom panel corresponds to a toy CIB experiment with 1° FWHM. The cross correlation measurement is mainly limited by the angular resolution of CIB experiment at low z and limited amount of galaxies at high z .

$C_{\text{IR,G}}$ can be measured with $\sim 10\%$ accuracy at 10° scales and $z \lesssim 0.6$ for a combination of FIRAS and SDSS (Fig. 2). In these ranges, the error of cosmic variance dominates. To beat down the cosmic variance, higher angular resolution CIB experiment is required, which can probe smaller angular scales (Fig. 2). Since the median redshift of SDSS galaxies is $z_m \sim 0.5$, where most correlation signal should come from, one expects the optimal measurement to be at $z \sim 0.5$ (Fig. 2). Since only a small fraction of SDSS galaxies lies at $z \gtrsim 1$, the correlation signal is weak and the short noise of galaxy distribution is large. Thus the correlation measurement becomes noisy. To measure the cross correlation at $z \gtrsim 1.5$, a deeper galaxy survey is needed.

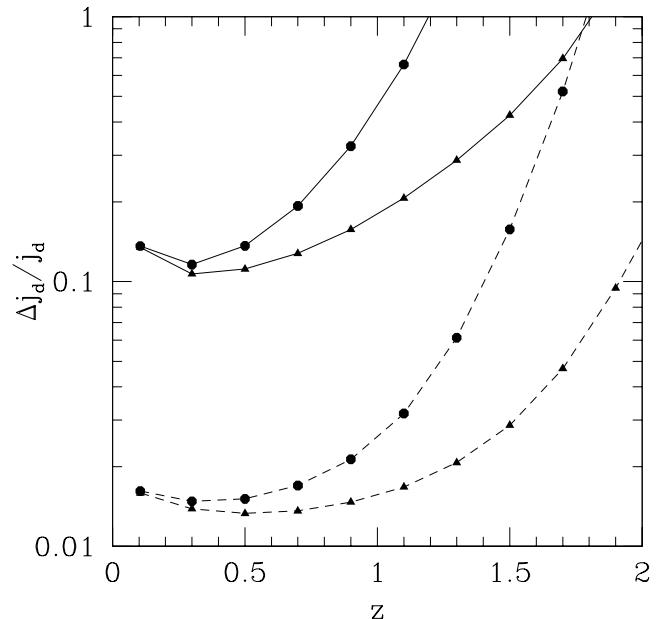


FIG. 3.— The estimated statistical errors of \bar{j}_d measured from the CIB-galaxy correlation. Data points connected with solid lines correspond to FIRAS and those connected with dash lines correspond to a toy CIB experiment with 1° FWHM. Filled circle points correspond to SDSS with a Galaxy median redshift $z_m = 0.5$ and filled triangle points corresponds to a toy galaxy survey with $z_m = 1.0$ and the same amount of galaxies at low redshift as SDSS. We have assumed the 3D correlation of IR emissivity-galaxy to be known.

Given $\Delta_{j_G}^2$, $\bar{j}_d(\bar{z})$ can be directly inferred from $C_{\text{IR,G}}$ (Eq. 6). The accuracy of the measured $\bar{j}_d(\bar{z})$ is then determined by the accuracy of $C_{\text{IR,G}}$ measurement. We approximate the relative error of the inferred $\bar{j}_d(z)$ as the minimum $\Delta C_{\text{IR,G}}/C_{\text{IR,G}}$. The result estimated by this somewhat arbitrary simplification should not deviate from that of a sophisticated analysis by a factor ~ 2 (Fig. 2), so it is sufficient for our purpose. Currently, the extraction of $\bar{j}_d(z)$ is mainly limited by the finite depth of the galaxy survey (Fig. 3). FIRAS+SDSS could measure the dust emissivity \bar{j}_d with $\sim 10\%$ accuracy at $z \lesssim 0.7$. For higher z , the measurement becomes noisy quickly. The accuracy of \bar{j}_d measurement is limited by the angular resolution of CIB experiment at low z and the amount of galaxies in galaxy surveys at high z . Combining a possible future CIB experiment with 1° FWHM and a deeper galaxy survey with median redshift $z_m = 1.0$, one may probe \bar{j}_d and

³ Private communication with Dale J. Fixsen.

the star formation history to $z \sim 1.5$ with several percent statistical errors.

Since our redshift bins are $\Delta z \sim 0.2$ and one does not expect strong evolution of Δ_{jG}^2 over these redshift ranges, the above analysis does not require precision measurement of galaxy redshifts. Photometric redshift can be measured with $\sigma_z/(1+z_{\text{spec}}) \sim 0.04$ at $z < 6$ (Massarotti, Iovino, Buzzoni, & Valls-Gabaud 2001), so the error of photo- z should not affect our result significantly.

The extraction of \bar{j}_d is based on known Δ_{jG}^2 , which is in principle an observable. Since at sufficiently large scale, the cross correlation coefficient of j_d and galaxies is unity, combining the mean CIB flux and CIB auto correlation measurement and galaxy Δ_G^2 measurement, \bar{j}_d and Δ_{jG}^2 can be determined simultaneously given the cosmology. However, the feasibility of this approach relies on future accurate removal of foregrounds, so we postpone its discussion in this paper. Furthermore, as we will show in §4, the measurement of CIB-ISW cross correlation is able to determine the mean bias of j_d and thus Δ_{jG}^2 .

4. CIB-CMB CROSS CORRELATION

Recent successful detections of the cross correlation between WMAP and galaxies (Fosalba & Gaztanaga 2003; Fosalba, Gaztañaga, & Castander 2003; Scranton et al. 2003; Afshordi, Loh, & Strauss 2003) present a powerful way to constrain cosmology, especially dark energy (through the ISW effect). But current galaxy surveys are either limited by finite sky coverage (For APM, 4300 deg² and for present SDSS, 3400 deg²) or by finite survey depth (For 2MASS, $\langle z \rangle \lesssim 0.1$). This limits current detections to $\lesssim 3\sigma$ level. To bypass these limitations, one can cross correlate CMB with other cosmic backgrounds, to reduce cosmic variance and to amplify cross correlation signal. One choice is the X-ray background (XRB). But the measurement of WMAP and the all sky XRB survey ROSAT fails to show any significant correlation (Diego, Silk, & Sliwa 2003). On one hand, XRB is dominated by AGNs, which mainly concentrate to high redshift. On the other hand, ISW mainly comes from low redshift where Ω_m deviates significantly from 1. At degree scale, which is the finest scale WMAP+ROSAT can probe, SZ contribution also mainly comes from low redshift (see, e.g., Zhang & Pen (2001)). So one does not expect a strong correlation between WMAP and ROSAT. Another choice is the cosmic radio background (CRB). Since the Milky Way is a strong synchrotron radiation source, which has a similar spectral index as the CRB synchrotron component, the subtraction of CRB foregrounds is difficult. Without a robust subtraction of CRB foregrounds, the tight correlation between galactic foregrounds (For CMB, synchrotron and free-free emission, Bennett et al. (2003)) may bias the CIB-CMB correlation measurement significantly. On the other hand, the origin of CRB is difficult to predict analytically. The synchrotron component of CRB associates with magnetic field, which is poorly understood. The thermal component of CRB associates with HII regions generated by massive star formation and is hard to predict too. So, even if the intrinsic cross correlation is detected, it would be hard to interpret. MeV cosmic γ -ray background (CGB) is expected to have a tight correlation with the large scale structure, but current CGB experiments

may be too noisy to detect any significant cross correlation with CMB (Zhang & Beacom 2004).

SCIB traces star forming galaxies, which have strong correlation with gravitational potential (ISW) and gas thermal pressure (SZ effect). The modeling of SCIB is relatively straightforward, as discussed in previous sections. So, the interpretation of CIB-CMB correlation is relatively robust. Thus, SCIB-CMB cross correlation is a good way to measure the ISW effect and the SZ effect. The detection of such cross correlation signal is observationally feasible, as implied by the successful detection of COBE-FIRAS correlation (Burigana & Popa 1998).

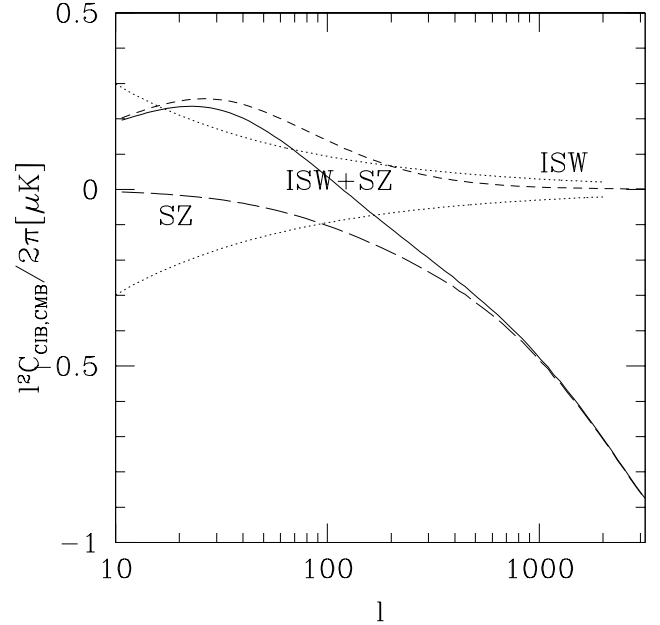


FIG. 4.— CIB-CMB cross correlation. The SZ effect is estimated in the Rayleigh-Jeans regime. The dot lines are the upper limit of systematic errors caused by the CIB and the CMB dust foreground correlation. This estimation assumes no foreground reduction in CMB maps and assumes perfect foreground correlation. With reasonable CMB foreground removal, the systematic error can be reduced by a factor of 10.

4.1. CIB-ISW cross correlation

The cross correlation power spectrum of ISW-CIB is given by

$$\frac{l^2}{2\pi} C_{\text{IR,ISW}} \bar{I} = \int \frac{\bar{j}_d}{4(1+z)^2} \frac{2a\chi}{c^3 l} \Delta_{j\phi}^2 \left(\frac{l}{\chi}, z \right) d\chi. \quad (13)$$

If assuming a bias model ($\delta_j = b_j \delta$), we obtain

$$\begin{aligned} \Delta_{j\phi}^2(k, z) &= \frac{3}{2} H_0^2 b_j \left(\frac{d}{dt} \left(a^{-1} \frac{\Delta_\delta^2}{k^2} \right) - a^{-1} \frac{\Delta_\delta^2}{2k^2} \right) \\ &\simeq \frac{3}{2} H_0^2 b_j \frac{d}{dt} \left(\frac{D}{a} \right) \frac{\Delta_\delta^2}{Dk^2} : \text{linear regime} \end{aligned} \quad (14)$$

Here, D is the linear density growth factor, calculated by the fitting formula of Carroll, Press, & Turner (1992). a is the scale factor. H_0 is the present Hubble constant. The power of $\Delta_{j\phi}^2$ concentrates on large scale due to the k^2 term in the denominator, thus the ISW effect dominates the CIB-CMB correlation at large angular scale ($l \lesssim 100$)

and drops to zero quickly toward small scale (Fig. 4). The correlation amplitude reaches $\sim 0.5\mu\text{K}$ at $l \sim 20$. One bonus of ISW-CIB correlation is that it gives the mean b_j averaged over redshift.

4.2. CIB-SZ cross correlation

The CIB-SZ cross correlation power spectrum in the Rayleigh-Jeans regime is given by

$$\frac{l^2}{2\pi} C_{\text{IR,SZ}\bar{I}} = -2 \int \frac{\bar{j}_d}{4} \frac{\bar{p}_e}{m_e c^2} \sigma_T \frac{\chi}{l} \Delta_{j_p}^2 \left(\frac{l}{\chi}, z\right) d\chi. \quad (15)$$

Here, $\Delta_{j_p}^2$ is the cross correlation power spectrum (variance) of δ_j and $\delta_p \equiv p_e/\bar{p}_e - 1$. We calculate the gas density weighted temperature \bar{p}_e by the continuum field model (Zhang & Pen 2001), which agrees with ΛCDM and self similar hydro simulations very well (Zhang, Pen & Trac 2004). This model predicts a mean temperature decrement $5.0\mu\text{K}$. The modeling of $\Delta_{j_p}^2$ is much more complicated. For simplicity, we assume δ_p traces dark matter overdensity with a constant bias $b_p = 5$, as predicted by Zhang & Pen (2001). The CIB-SZ correlation dominates at $l \gtrsim 100$. At one degree scale ($l \sim 300$), the cross correlation amplitude reaches $-0.3\mu\text{K}$ (Fig. 4).

With a possible future CIB experiment of (sub)degree angular resolution, the CIB-SZ cross correlation can be measured. The SZ effect is sensitive to various thermal heating processes such as SN feedback and quasar feedback. The O and B star formation responsible for SCIB is also responsible for SN feedback on the intergalactic medium, so the measurement of CIB-SZ cross correlation helps to constrain the role of SN feedback on the SZ effect.

4.3. Observational feasibility

Since we will utilize (almost) full sky data, we expect a factor of 3-4 decrease in the sample variance with respect to current WMAP+galaxy measurement. Furthermore, Interplanetary dust does not correlate with CMB foregrounds. The main obstacle of CIB-CMB cross correlation measurement comes from the correlations of CIB and CMB galactic foregrounds, mainly the galactic dust foregrounds. But such correlations concentrate on large scales. The power spectrum of CIB galactic dust foreground scales as $C_l \propto l^{-3}$. CMB galactic foregrounds have a combined power spectrum $C_l \propto l^{-2}$ (Bennett et al. 2003). These foreground correlations degrade the detection of the ISW effect, but has only minor effect on the detection of the SZ effect. Furthermore, one can avoid the galactic plane to minimize foregrounds.

We can estimate the upper limits of the systematic errors caused by foreground correlations. For the WMAP W band, the only non-negligible foreground is galactic dust emission with a flat power spectrum $C_l l^2 / (2\pi) \simeq 50\mu\text{k}^2$ (Fig. 10, Bennett et al. (2003)). This foreground strongly correlates with the CIB galactic foreground, which has a power spectrum $C_l \simeq (10 \text{ nWm}^{-2}\text{sr}^{-1})^2 l^{-3}$ (§3.2). Without any foreground removal, the systematic error introduced by foreground correlations prohibits the CIB-CMB correlation measurement at $l \lesssim 20$, but it still leaves a window at $20 \lesssim l \lesssim 60$ for the CIB-ISW cross correlation detection. Its effect to the CIB-SZ cross correlation measurement at $l \gtrsim 200$ is negligible (Fig. 4).

Current foreground removal method using multi-frequency maps can reduce CMB foreground contaminations in the CMB power spectrum by more than 90%. For cleaned WMAP map at W band, foreground only contributes 0.4% of the CMB power spectrum (Bennett et al. 2003). Since maps used for foreground removal correlate with SCIB, in principle, the foreground removal process may introduce false correlation signal with SCIB or lose correlation signal. But The ISW contribution to CMB at $l \sim 10$ and the SZ contribution to CMB at $l \gtrsim 300$ are much larger than 0.4%, thus the CMB signal responsible for CMB-CIB correlation do survive after the foreground removal process. so we can neglect such complexity in the cleaned map. Thus using cleaned CMB map, one expect a factor of ~ 10 reduction in the systematic errors.

FIRAS has an angular resolution $\sim 5^\circ$ and thus can probe $l \sim 20$. Around such scales, the statistical error of CIB-CMB correlation measurement is $\simeq \sqrt{2/(2l+1)\Delta l} \lesssim 10\%$ and the systematic error is $\lesssim 10\%$ using cleaned WMAP W band map. So, combining WMAP and FIRAS, one expects $\sim 20\%$ accuracy in the CMB-CIB cross correlation measurement.

5. CONCLUSION

Cosmic infrared background (CIB) traces the large scale structure of the universe and contains plenty of information of the star formation history. But overwhelming foregrounds prohibit its precision measurement. By cross correlating cosmic infrared background with galaxies, one can eliminate CIB foregrounds, minimize and localize background contaminations and directly obtain redshift information of CIB sources from galaxy photometric redshift. Since one does not rely on spectral information to extract redshift information of CIB sources, one only needs to estimate the integrated CIB, which is directly determined by star formation rate through the energy conservation and is thus fairly model independent.

The CIB-galaxy cross correlation at degree scale is $\sim 10\%$ and can be measured with 10% accuracy. We estimated that, the cross correlation could enable a direct and statistically robust measurement of star formation rate with 10% to $z \lesssim 1.5$. With our model based on the integrated CIB intensity, we predict that the cross correlation between the CIB and the CMB is about $0.5\mu\text{K}$ at 10° scale (the ISW effect), changes sign at several degree scale and reaches $\sim -0.3\mu\text{K}$ at one degree scale (the SZ effect). We argue that this cross correlation is observationally feasible. Such measurement would constrain the amount of dark energy by the ISW effect, the amount of the thermal energy of the universe by the SZ effect and provide further constraint on the clustering property of SFG and make our CIB model self consistent.

Acknowledgments: The author thanks an anonymous referee for many helpful comments. The author thanks Albert Stebbins and Lam Hui for helpful discussion and thanks Dale J. Fixsen for explaining FIRAS beam. This work was supported by the DOE and the NASA grant NAG 5-10842 at Fermilab.

REFERENCES

- Afshordi, N., Loh, Y., & Strauss, M. A. 2003, ArXiv Astrophysics e-prints, astro-ph/0308260
- Baugh, C. M. & Efstathiou, G. 1993, MNRAS, 265, 145
- Bennett, C. L. et al. 2003, ApJS, 148, 97
- Bond, J. R., Carr, B. J., & Hogan, C. J. 1986, ApJ, 306, 428
- Brown, M. J. L., Boyle, B. J., & Webster, R. L. 2001, AJ, 122, 26
- Burigana, C. & Popa, L. 1998, A&A, 334, 420
- Carroll, S. M., Press, W. H., & Turner, E. L. 1992, ARA&A, 30, 499
- Diego, J. M., Silk, J., & Sliwa, W. 2003, MNRAS, 346, 940
- Dodelson, S. et al. 2002, ApJ, 572, 140
- Draine, B. T. & Lee, H. M. 1984, ApJ, 285, 89
- Fixsen, D. J., Dwek, E., Mather, J. C., Bennett, C. L., & Shafer, R. A. 1998, ApJ, 508, 123
- Fosalba, P. & Gaztanaga, E. 2003, submitted to PRL, astro-ph/0305468
- Fosalba, P., Gaztañaga, E., & Castander, F. J. 2003, ApJ, 597, L89
- Genzel, R. & Cesarsky, C. J. 2000, ARA&A, 38, 761
- Giavalisco, M., Steidel, C. C., Adelberger, K. L., Dickinson, M. E., Pettini, M., & Kellogg, M. 1998, ApJ, 503, 543
- Haas, M., Chini, R., Meisenheimer, K., Stickel, M., Lemke, D., Klaas, U., & Kreysa, E. 1998, ApJ, 503, L109
- Haiman, Z. & Knox, L. 2000, ApJ, 530, 124
- Hauser, M. G. & Dwek, E. 2001, ARA&A, 39, 249
- Hippelein, H. et al. 2003, A&A, 402, 65
- Karimabadi, H. & Blitz, L. 1984, ApJ, 283, 169
- Knox, L., Cooray, A., Eisenstein, D., & Haiman, Z. 2001, ApJ, 550, 460, L1
- Lilly, S. J., Le Fevre, O., Hammer, F., & Crampton, D. 1996, ApJ, 460, L1
- Lisinfeld, U., Voelk, H. J., & Xu, C. 1996, A&A, 306, 677
- Madau, P., Pozzetti, L., & Dickinson, M. 1998, ApJ, 498, 106
- Massarotti, M., Iovino, A., & Buzzoni, A. 2001, ApJ, 559, L105
- Massarotti, M., Iovino, A., Buzzoni, A., & Valls-Gabaud, D. 2001, A&A, 380, 425
- Miville-Deschênes, M.-A., Lagache, G., & Puget, J.-L. 2002, A&A, 393, 749
- Sachs, R. K. & Wolfe, A. M. 1967, ApJ, 147, 73
- Sanders, D. B. & Mirabel, I. F. 1996, ARA&A, 34, 749
- Scranton, R. et al. 2003, submitted to PRL, astro-ph/0307335
- Sheldon, E. S. et al. 2003, ArXiv Astrophysics e-prints, astro-ph/0312036
- Smith, R. E. et al. 2003, MNRAS, 341, 1311
- Song, Y., Cooray, A., Knox, L., & Zaldarriaga, M. 2003, ApJ, 590, 664
- Spergel, D. N. et al. 2003, ApJS, 148, 175
- Wright, E. L. 1998, ApJ, 496, 1
- Wright, E. L. 2003, astro-ph/0306058
- Zeldovich, Y. B. & Sunyaev, R., 1969, Ap&SS, 4, 301
- Zhang, P. & Pen, U. 2001, ApJ, 549, 18
- Zhang, P., Pen, U., & Wang, B. 2002, ApJ, 577, 555
- Zhang, P. & Beacom, J., 2004, astro-ph/0401351.
- Zhang, P., Pen, U., & Trac, H. 2004, astro-ph/0402115.